Natural Colorants Induce the Drug Release from Fast Dissolving Tablets

Esra Tariq Bayrakdar [1], Sharad Visht [1*], Duran Kala [2], Saya Ameer [1], Ahmad H. Ibrahim [1], Sawsan S. Al-Rawi [3], Samir Bhargava [4], Abhijeet Ojha [5]

Abstract

Background: The use of fast-dissolving tablets (FDTs) presents a promising solution to the challenges faced by certain patient populations, such as children and geriatric patients. FDTs offer rapid disintegration and dissolution in the oral cavity, facilitating drug absorption without the need for water, thus improving dosing accuracy and therapeutic outcomes. This study investigated the impact of hydrophilic and hydrophobic colorants on drug release from FDTs, utilizing Fluorouracil (5-FU) as a model drug and various natural pigments as colorants. Method: The research methodology involved the extraction and characterization of pigments from Opuntia ficus-indica fruits and Nyctanthes arbor-tristis flowers, followed by pre-formulation studies of 5-FU and formulation of FDTs using a direct compression method. Various evaluation parameters were employed to assess the physicochemical properties and performance of the FDTs. Results: The results indicated that the yield of pigments extracted from the fruits and flowers met acceptable standards, with FTIR analysis confirming their chemical composition. Pre-formulation studies of 5-FU revealed its physical and chemical characteristics, ensuring compatibility with excipients. The FDTs exhibited desirable properties such as uniform thickness, drug content uniformity, and acceptable weight variation, hardness, and friability. Moreover, the FDTs demonstrated rapid disintegration, dissolution, and water absorption, along with satisfactory wetting time and in-vitro drug release profiles. Conclusion: FTIR and DSC studies confirmed the absence of drug-excipient interactions, ensuring the stability and integrity of the formulations. Overall, the incorporation of hydrophilic and hydrophobic colorants did not significantly affect the performance of the FDTs, indicating their suitability for use in pharmaceutical formulations.

Keywords: 5FU, Fast Dissolving Tablets, Hydrophilic Colorants, Hydrophobic Colorants, Pigment Extraction, FTIR Characterization

Significance | This study showed the impact of hydrophilic and hydrophobic colorants on drug release, crucial for improving palatability and therapeutic efficacy of fast dissolving tablets.

*Correspondence. Sharad Visht, Pharmacy Department, Tishk International University, Erbil, Kurdistan Region, Iraq. Contact: +964-7511644562
E-mail: sharad.visht@tiu.edu.iq

Editor Md Shamsuddin Sultan khan, And accepted by the Editorial Board Apr 12, 2024 (received for review Feb 25, 2024)

Introduction

Tables are solid dosages forms that are most frequently used and accepted in large population of patients, but children and geriatric patients sometimes faces difficulties to swallow the solid oral dosage forms like hard/soft gelatin capsules and tablets. Even these formulations require some volume of water for administration that may be sometimes unavailable, like in travel or active working people in industries. This may result in improper dosing, therapeutic monitoring of drug. The fast disintegration/ dissolving tablets (FDTs) may be an alternative to resolve these problems and to meet the required therapeutic demands. (Kozarewicz, 2014) (Hajjar et.al., 2007; Zhang et.al., 2002; Tumuluri, 2022, Überall et.al., 2011).

The FDTs become popular around the world as these can mask the

Author Affiliation.
[1] Pharmacy Department, Tishk International University, Erbil, Kurdistan Region, Iraq.
[2] Dentestry Department, Tishk International University, Erbil, Kurdistan Region, Iraq.
[3] Biology Education Department, Tishk International University, Erbil, Kurdistan Region, Iraq.
[4] IPR Cell, DIT University, Dehradun, Uttarakhand, India.
[5] Amrapali Institute of Pharmacy and Science Haldwani, Uttarakhand, India.

Please cite this article.
Esra Tariq Bayrakdar et al.. (2024). Natural Colorants Induce the Drug Release from Fast Dissolving Tablets, Journal of Angiotherapy, 8(4), 1-12, 9622

bitter taste of drug, provide better drug absorption of poorly aqueous soluble drug from buccal cavity/ esophagus/ stomach by rapid disintegration/ dissolution and doesn't require water for drug administration in body. FDTs disintegrate/ dissolve in the mouth spontaneously with rapid de-aggregation as FDTs encounter saliva and turns into solution that allow better absorption of drug through membranes during deglutition. The direct absorption of some drug fraction through the oral mucosa results in possibility of drug movement to systemic circulation, bypassing the GIT and first-pass effect of the drug. The FDTs may be highly porous/ soft-moldable matrices/ compact formulation at low compression force to lower the hardness and to achieve fast disintegration of tablet. (PS et al. 2022; BI et al., 1996; Bond, 1998; European Pharmacopoeia 5th Ed) The composition of FDT includes fillers, super disintegrants, binder, glidant, lubricant, sweeteners, and flavors. The sweeteners and flavors improve the palatability and acceptance of these formulations. Taste masking of bitter drugs containing FDTs are generally achieved by microencapsulation, complexation, fluidized-bed coating, freeze-drying and supercritical fluids for taste-masking purposes. Several techniques are used to prepare FDTs are lyophilization, sublimation, spray drying, tablet molding, solid deposition, use of super disintegrants, use of effervescent combinations. (Ratner et.al., 2000; Ayenew et.al., 2009; Hirlekar et.al., 2009; Soni et.al., 2008)

The present research focused on the effect of hydrophilic and hydrophobic colorant on drug release as the colorants adsorb on the phases of drug and may interfere with the dissolution. The *Fluorouracil* (*5-FU*) was used as a model drug; pigment from opuntia fruits (*Opuntia ficus-indica*), Parijat flower (*Nyctanthes arbor-tristis*) and amaranth were used as hydrophilic colorants and curcumin (turmeric) as hydrophobic colorant.

2. Material and methods

The 5-*fluorouracil* (*5-FU*) was procured form FINKEM (Batch No. 374147), Erbil, Iraq. The citric acid was procured form Scharlau, sodium bicarbonate, sodium stearate from TEKKIM, polyvinyl pyrolidone K90, sucrose, amaranth from FINKEM. The curcumin was a gift sample from Indian Glycols Limited (Ennature Biopharma Division), Noida, Utter Pradesh. The lemon oil was procured from Bahar Co. Industry at Sulaymania. The pigments from *Opuntia ficus-indica* fruits and *Nyctanthes arbor-tristis* flowers were extracted. The curcumin was a hydrophobic pigment. The amaranth was hydrophilic colorant. The pigments obtained from *Opuntia ficus-indica* fruit, *Nyctanthes arbor-tristis* flowers were hydrophilic pigments. All chemicals were of analytical grade and were procured from commercial sources.

2.1. Collection and Authentication

The fruits of *Opuntia ficus-indica* and flowers of *Nyctanthes arbor-tristis* were authenticated from Botanist, Prof. Pulok Mondol at HAPPRC Unit, Department of Botany, Hemwati Nandan Bahuguna Central (Gharwal) University, Srinagar, Uttrakhand, India (Ref: Plant/Regis/113-114/20200929).

2.2. Methodology

2.2.1. Extraction of pigment from *Opuntia ficus*-indica fruits and *Nyctanthes arbor-tristis* flowers:

Accurately weighed 200 g of *Opuntia ficus-indica* fruit was smashed using a mixer grinder and allowed to be soaked with ethanol in 1 L conical flask. The mechanical stirrer was used to mix the mixture for maximum extraction of pigments for 1 hour. Filter the mixture using qualitative filter paper (size 102), centrifuge at 10000 rpm for 5 minutes and finally dried using freeze drier. The pictorial representation of the extraction procedure is given in Supp. Figure-1 (A). (Santos et.al., 2022; Fernández-López et.al., 2022; Scarano et al., 2020; Sepúlveda et.al., 2007)

The pigment from Nyctanthes arbor-tristis flowers was placed in a thimble and packed in Soxhlet apparatus. The ethanol was used for extraction of solvent. Mixture was placed in freeze drier. The pictorial representation of the extraction procedure is given in Supp Figure-1 (B). (Tripathi et.al., 2012; Shrivastava et.al., 2018; Bijauliya et al., 2021, Singh et.al., 2021)

2.2.2. Characterization of pigments from *Opuntia ficus*-indica fruits and *Nyctanthes arbor-tristis* flowers:

2.2.2.1. Yield of pigments

The yield of pigments extracted from the *Opuntia ficus*-indica fruits and *Nyctanthes arbor-tristis* flowers were determined. (Ngamwonglumlert et.al., 2017)

2.2.2.2. FTIR study

The FTIR study was performed using Fourier transform infrared spectrophotometry (IRAffinity-1S, Shimadzu). FTIR is used for the identification of different type of bonds and functional groups in a pure molecule or a mixture. The FTIR of curcumin and amaranth was also performed. (Visht et.al., 2018)

2.2.3. Pre-formulation study of 5-*fluorouracil* (*5-FU*)

Pre-formulation studies included examination of physical composition, organoleptic properties of the drug, melting point, DSC, UV analysis, FTIR, drug and drug compatibility by FTIR spectrometry etc. (Aulton et.al., 2013)

2.2.3.1. Organoleptic properties

5-Fluorouracil was characterized based on organoleptic properties (color, taste, and odor) and compared with literature. (Visht et.al., 2015)

2.2.3.2. Physical characterization

Physical characterization includes determination of physical state like amorphous or crystalline form. (Srivastava et.al, 2010)

2.2.3.3. Melting point

The melting point is measured to identify the compound and it also reflects the solubility and purity characteristics of component. The capillary fusion method was used to determine the melting point of 5-Fluorouracil. The digital capillary melting point apparatus was used to determine the drug point and was measured using sodium bicarbonate AR and L-ascorbic acid AR. The melting point of 5-Fluorouracil was determined in a separate capillary tube using digital melting material and the melting point was compared to the volume of the literature. (Visht et.al., 2015)

2.2.3.4. Loss on drying:

The accurately weighted 10 g 5-Fluorouracil was allowed to dry in hot air oven, pre-adjusted at 105±1°C, until two constant readings were recorded. (Visht et.al., 2015)

2.2.3.5. UV Spectrophotometric study

UV-Spectrophotometric studies were performed using a double beam U. V. Spectrophotometer (Cintra 2020, GBC Scientific Equipment). The stock solution (1 mg/ml) was prepared in phosphate buffer solution (pH 7.4) and dilutions (2, 4, 6, 8, 10, 12, 14, 16, 18, 20 µg/ml) were prepared. The λ_{max} was determined; absorbance of all prepared dilution was measured, and calibration curve was plotted absorbance vs concentrations (µg/ml). (Sharma et.al., 2012)

2.2.3.6. FTIR study

The FTIR spectroscopy studies were performed as per discussed above. (Visht et.al., 2016)

2.2.3.7. DSC

The differential scanning calorimetry (DSC) was performed using calorimeter (DSC-60APlus, Shimadzu) using a pure sample of 5-FU. The drug sample (5-Fluorouracil) was placed in an aluminum pan and closed using a lid. The drug (5-Fluorouracil) loaded pan was placed on sample tray and DSC was programmed to be heated to 300°C. The holding temperature was 10°C. The nitrogen was used during study and flow rate was 10 ml/min. The DSC data was recorded that showed the output as a graph of heat (mW) vs time (Minutes) vs temperature (°C) that was converted into heat (mW) vs temperature (°C). (P et.al., 2012)

2.2.3.8. Drug-Excipient Interaction by FTIR

Drug-excipient interaction studies were performed using FTIR (IRAffinity-1S, Shimadzu). The individual FTIR of drug, excipients and formulations were determined to find the drug excipient compatibility. The FTIR spectroscopy were performed as per discussed above. (Visht et.al., 2018)

2.2.3.9. Drug-Excipient Interaction by Differential Scanning Calorimetry (DSC) Study

The FTIR spectroscopy were performed as per discussed above. (Wolska et.al., 2020)

2.2.4. Preparation of Fast Dissolving Tablets by Direct Compression Method

The direct compression method was used to prepare the FDTs of *fluorouracil* (*5-FU*). All the ingredients were passed through #60 separately for uniformity of particle size distribution. Accurately weighed quantities as described in Table-1 were mixed in mortar pestle and grinded for homogenous mixing. The mixed powder was fed into hopper of electrically driven single punch tablet punching/compression machine using 8 mm diameter, concave punch and 8 mm die to prepare the tablets of 350 mg weight. (Shirsand et al., 2010)

2.2.5. Evaluation Preparation of Fast Dissolving Tablets

The powdered blend was used to determine the bulk density, true density, pore volume, porosity, flow properties and compression indexes. (Patel et.al, 2020)

2.2.5.1. Bulk Density (ρ_d):

The bulk density (ρ_d) was examined by pouring the powdered mixture into a measuring cylinder. The weight of powder (M) and bulk volume were measured. The bulk density was calculated using the following formula. (Mehra et al., 2021)

$\rho_d = M/V_b$

Where,

ρ_d = Bulk density

M = Mass of powder

V_b = Bulk volume

2.2.5.2. True Density or Tapped Density (ρ_t):

The measuring cylinder containing a fixed amount of powder was tapped at 1250 tapping from fixed height (3 mm). The least volume (V_t) occupied by powder in measuring cylinder and the weight (M) of the powder blend was measured. The tapped density (ρ_t) was calculated as per formula given below. (Bhimte et.al, 2007)

$\rho_t = M/V_t$

Where,

ρt = True density

M = Mass of powder

V_t = True volume

2.2.5.3. Void / Pore Volume:

The void volume (ml) was determined by subtracting bulk volume and tapped volume as formula given below: (Mohan et.al., 2015)

Void volume (ml) = Bulk volume - Tapped volume

$V_0 = (V_b - V_t)$

Where,

V_0 = Void volume

V_b = Bulk volume

V_t = True volume

2.2.5.4. Porosity:

The porosity is the volume of space between the solid particles of the powder against volume of powder. Porosity is calculated using the following formula: (N et.al., 2011)

Porosity = Void volume / Total volume

$T = (V_0 / V_t)$

Where,

V_0 = Void volume

V_b = Bulk volume

V_t = True volume

2.2.5.5. Flow Properties by Angle of repose:

The funnel method was used to determine the angle of repose. Accurately weighed amount of powder was placed in a funnel and allows flowing down freely. The angle of repose was calculated using the following equation: (Sharma et.al., 2010)

$\tan \theta = h/r$

Various ranges of flow ability and angle of repose were given in Table- 2.

2.2.5.6. Hausner's ratio

The ratio of tapped density to bulk density is Hausner's ratio. Generally, the better powder flow property is related to lower the value of Hausner's ratio. Hausner's ratio is calculated by the following formula: (Heer et al., 2019)

Hausner's ratio = Tapped Density/Bulk Density

Lower Hausner ratios (<1.25) indicate better flow properties than higher ratios (>1.25).

Various ranges of Hausner's ratio are given in Table-3.

2.2.5.7. Carr's Compressibility index

Carr's index is a percentage ratio of the difference between tapped density and bulk density against tapped density as shown in below formula: (Balata et.al., 2016)

Carr's index = (Tapped Density-Bulk Density) *100/ Tapped Density

Various ranges of Carr's Compressibility index are given in Table-4.

2.2.6. Evaluation of Fast Dissolving Tablets

2.2.6.1. Uniformity of Thickness

The 10 tablets were evaluated for thickens by placing the tablet between the anvils of the Venire calipers individually. (A et.al., 2010)

2.2.6.2. Drug Content Uniformity

The 20 tablets were weighed and crushed into powder. The grounded powder equivalent to 5 mg of the drug was weighed, diluted, and analyzed using a double beam U. V. Spectrophotometer (Cintra 2020, GBC Scientific Equipment) at 210 nm. (SA et al., 2020)

2.2.6.3. Weight Variation Test

Randomly 20 tablets were sampled and both individual and average weight of tablets were determined. The weight of individual tablet against average weight of tablet were compared. If the comparison of weight variation lies within the I.P limits, tablets passed the weight variation test. (Sharma et.al., 2013)

2.2.6.4. Hardness Test

The tablet hardness affects the disintegration and dissolution times of tablets and the absorption and bioavailability. It was measured as force/load/pressure required to crush a tablet when placed between two edges. The YD-1 Tablet Harness Tester (Made: Tian Jin Optical Instrumentation Factory) was used to measure the hardness of tablet in Newton. (Patel et.al., 2020)

2.2.6.5. Friability Test

The CS-2 Friability Tester was used to measure the friability of the tablets. The combined effect of abrasions and shock was measured in a plastic chamber that revolves at 25 rpm. The tablets were drop from 6 inches' height on each revolution. A pre-weighed tablets was placed in the friabilator and revolved for 100 revolutions. A soft muslin cloth was used to de-dust the tablets and teeters were reweighed. The friability (F%) was calculated by following formula: (Panigrahi et.al, 2022)

$F = (W_0) - (W) * 100 / (W_0)$

Where,

W_0 = Initial weight of the tablets before the test

W = Weight of the tablets after the test

2.2.6.6. Water Absorption

A tissue paper was twice folded and placed in a small Petri dish contained 6 mL of water. The tablet was placed on this paper. The time required for complete wetting of tablet was examined and the weight of wet tablet was then measured. The water absorption ratio (R) was calculated using the following equation: (Corveleyn et.al, 1997)

$R = 100 (W_a - W_b)/W_b$

Where,

R = Water absorption ratio

W_a = Initial weight of tablet

W_b = Weight of wet tablet

2.2.6.7. Wetting Time

A tissue paper was twice folded and placed in a petri plate contained 6 mL of water (37°C). The tablet was placed on the tissue paper. The time (seconds) required for the complete wetting of the tablet was measured. (Bharkatiya et.al., 2018)

2.2.6.8. *In-vitro* Disintegration Time

The disintegration time was measured by disintegration test apparatus by placing a tablet in each tube of the dissolution apparatus. The basket was immersed in a pre-heated water bath maintained at 37±0.20°C to measure the disintegration time. (Parkash et al., 2011)

2.2.6.9. *In-vitro* Dissolution Studies

The *in-vitro* dissolution test was conducted in triplicate. The USP dissolution apparatus Type-II (Paddle type) (Model: DIS8000) was used for the *in-vitro* dissolution studies. The 900 ml phosphate buffer (pH 6.8) was used as the dissolution medium. The stirring speed was 100 rpm. Temperature of dissolution fluid was 37±0.5 ºC. The samples were withdrawn at 1, 5, 10, 15, 30, 45, 60, 75, 90 minutes time intervals and replaced with fresh volume of buffer. The absorbance of various collected samples was scanned at λ_{max} 210 nm a double beam UV Spectrophotometer. The percentage drug release was measured and the plotted % cumulative drug release vs time. [Bharkatiya et.al., 2018]

2.2.6.10. Drug release kinetics

The kinetics drug release was determined for all batches to know the best fit model and mechanism of drug release using BIT-SOFT 1.12.

2.2.6.11. Stability study:

The optimized batch of FDT formulation was placed for 7, 14, 21 and 28 days at 25±2ºC, 60±5%RH to analyze the drug content.

3. Results and Discussion

The yield of pigments extracted from *Opuntia ficus*-indica fruits and *Nyctanthes arbor-tristis* flowers were found to be 1.67±0.25%w/w and 1.83±0.36% w/w. The FTIR studies showed no drug excipient interaction and FTIR showed in Figure-2.

The FTIR of curcumin showed the of O-H stretching vibrations of phenolic hydroxyl groups at 3200-3500 cm^{-1}, aromatic C=C at 1490 cm^{-1}, alkenyl C=C stretch 1680-1620, phenolic C-O at 1246 cm^{-1}, C=O at 1725-1705 cm^{-1}, phenolic C-O stretch at ~1200, C-H methyl *asym./sym.* bending at 1470-1430/1380-1370 cm^{-1}, C-H stretch of (methoxy, methyl ether) O-CH_3 at 2850-2815 cm^{-1}, phenolic OH stretch at 3640–3530 cm^{-1}, methoxy C-H stretch (CH_3-O-) at 2820-2810 cm^{-1}.

The FTIR of amaranth showed the presence of aromatic C=C at 1490 cm^{-1}, alkenyl C=C stretch 1680-1620 cm^{-1}, C-O at 1246 cm^{-1}, C=O at 1725-1705 cm^{-1}, C-O stretch at ~1200 cm^{-1}, OH stretch at 3640-3530 cm^{-1}, C-H stretch at 2820-2810 cm^{-1}, C-OH stretching at 1079 cm^{-1}, C-S stretch at 705-570 cm^{-1}, -N=N- at 1630-1575 cm^{-1}, aromatic C-H stretch 3130-3070 cm^{-1}, C=C-C aromatic ring stretch 1615–1580 cm^{-1}/ 1510-1450 cm^{-1}/ 3130-3070 cm^{-1}, hydroxy group OH stretch (broad) at 3570-3200 cm^{-1}, C-C at 1300-700 cm^{-1}, aromatic combination bands (several) at 2000-1660 cm^{-1}, C-O stretch at 1150-1050 cm^{-1}, several aromatic C-H in-plane bend at 1225-950 cm^{-1} and several aromatic C-H out-of-plane bend at 900-670 cm^{-1}.

The FTIR of pigment obtained from *Opuntia ficus-indica* fruits showed the presence of C-H stretch at 2850-2815 cm^{-1}, C-H *asym./sym.* bending at 1470-1430/1380-1370 cm^{-1}, aromatic C=C at 1490 cm^{-1}, C=C stretch 1680-1620, C=C-C aromatic ring stretch 1615-1580 cm^{-1}/ 1510-1450 cm^{-1}/ 3130-3070 cm^{-1}, OH stretch (broad) at 3570-3200 cm^{-1}, C-C at 1300-700 cm^{-1}, C-O stretch at 1150-1050 cm^{-1}, several aromatic C-H in-plane bend at 1225-950 cm^{-1}, several aromatic C-H out-of-plane bend at 900-670 cm^{-1}, aromatic C-H stretch 3130-3070 cm^{-1}, C-S stretch at 705-570 cm^{-1}, C-OH stretching at 1079 cm^{-1}, C-H stretch at 2820-2810 cm^{-1}, OH stretch at 3640-3530 cm^{-1}, C-O stretch at ~1200 cm^{-1}, C-O at 1246 cm^{-1}, C=O at 1725-1705 cm^{-1}, aromatic C=C at 1490 cm^{-1}, alkenyl C=C stretch 1680-1620 cm^{-1}.

The FTIR of pigment obtained from *Nyctanthes arbor-tristis* flowers showed the presence of C-H stretch at 2850-2815 cm^{-1}, C-H *asym./sym.* bending at 1470-1430/1380-1370 cm^{-1}, aromatic C=C at 1490 cm^{-1}, C=C stretch 1680-1620, C=C-C Aromatic ring stretch 1615-1580 cm^{-1}/ 1510-1450 cm^{-1}/ 3130-3070 cm^{-1}, OH stretch (broad) at 3570-3200 cm^{-1}, C-C at 1300-700 cm^{-1}, C-O stretch at 1150-1050 cm^{-1}, several aromatic C-H in-plane bend at 1225-950 cm^{-1}, several aromatic C-H out-of-plane bend at 900-670 cm^{-1}, aromatic C-H stretch 3130-3070 cm^{-1}, C-S stretch at 705-570 cm^{-1}, C-OH stretching at 1079 cm^{-1}, C-H stretch at 2820-2810 cm^{-1}, OH stretch at 3640-3530 cm^{-1}, C-O stretch at ~1200 cm^{-1}, C-O at 1246 cm^{-1}, C=O at 1725-1705 cm^{-1}, aromatic C=C at 1490 cm^{-1}, alkenyl C=C stretch 1680-1620 cm^{-1}.

The FTIR of 5-FU showed the presence of C-F at 1150-1000 cm^{-1}, C=O at 1630-1635 cm^{-1}, C-N at 1410 cm^{-1}, N-H at 1649-1652 cm^{-1}, C=C at 1680-1620 cm^{-1}, C-H at 1485-1445/ 1350-1330 cm^{-1}. The FTIR of citric acid showed the presence of O-H (COOH) at 3491 cm^{-1}, C=O (COOH) at 1752 cm^{-1}, C-OH stretching at 1207 cm^{-1}, C-OH bending at 1169 cm^{-1}.

The FTIR of sodium bicarbonate showed the presence of OH at 3752 cm^{-1}, asymmetric CO_2 1734 cm^{-1}, symmetric CO_2 1259 cm^{-1}, C-OH 1171 cm^{-1}, C-OH 873 cm^{-1}, CO_2 bend 609 cm^{-1}, CO_2 wagging 533 cm^{-1}, CO_2 out of plan 787 cm^{-1}, OH out of plan 482 cm^{-1}.

The FTIR of sodium stearate showed the presence of C=O, C-OH, C-C, metal-carboxylate, and carboxylic acid (1698-1710 cm^{-1}. C-H stretching at 2954 cm^{-1}/ 2917 cm^{-1}/ 2848 cm^{-1}, COO^- stretching at 1577 cm^{-1}/ 1337 cm^{-1}.

The FTIR of *polyvinylpyrrolidone* showed the presence of O-H stretching at 3395 cm^{-1}, C-H stretching at 2951 cm^{-1}, C=O stretching at 1646 cm^{-1}/ 1424 cm^{-1}, C-N stretching at 1287 cm^{-1}/ 1166 cm^{-1}, strong C=O absorption peak from amide group at 1652 cm^{-1}, C-N group appeared at 1287 cm^{-1}, C–H stretching and bending vibrations were observed at 2800-3000 cm^{-1} and 1420-1460 cm^{-1}, respectively. OH at 3396 cm^{-1}, asymmetric CH_2 2950 cm^{-1}, symmetric CH_2 at 2922 cm^{-1} 2349 cm^{-1}, C=O at 1646 cm^{-1}, C-H 1373 cm^{-1}, CH_2 wagging 1286 cm^{-1}, C-N 1286 cm^{-1}, C-C 017 cm^{-1}, CH_2 1017 cm^{-1}, C-C 933 cm^{-1}, CH_2 843 cm^{-1}, N-C=O 572 cm^{-1}.

The FTIR of sucrose showed the presence of OH stretch (phenol) at 3500 cm^{-1}, tert-OH or phenols at 1100 cm^{-1}, mono sub alkenes C-H bond at 900 cm^{-1}, secondary alcohols at 1090 cm^{-1}, aromatic C=C or carboxylates at 1575 cm^{-1}, methyl at 2925 cm^{-1}, esters at 1175 cm^{-1}.

Table 1. Composition of FDT Batches

	Composition of Batches											
Ingredients	**FDT1**	**FDT2**	**FDT3**	**FDT4**	**FDT5**	**FDT6**	**FDT7**	**FDT8**	**FDT9**	**FDT10**	**FDT11**	**FDT12**
5-Florourasil (mg)	250	250	250	250	250	250	250	250	250	250	250	250
Citric acid (mg)	4	4	4	4	4	4	4	4	4	4	4	4
Sodium bicarbonate (mg)	7	7	7	7	7	7	7	7	7	7	7	7
Sodium stearate (mg)	1.5	1.5	1.5	1.5	1.5	1.5	1.5	1.5	1.5	1.5	1.5	1.5
Polyvinylpyrrolidone (mg)	5	5	5	5	5	5	5	5	5	5	5	5
Sucrose (mg) (q.s. 350 mg)	31	29	27	31	29	27	31	29	27	31	29	27
Lemon oil (mL)	0.5	0.5	0.5	0.5	0.5	0.5	0.5	0.5	0.5	0.5	0.5	0.5
Curcumin (0.01% methanolic solution) (mL)	1	3	5	0	0	0	0	0	0	0	0	0
Amaranth (0.01% methanolic solution) (mL)	0	0	0	1	3	5	0	0	0	0	0	0
Anthocyanin (0.01% methanolic solution) (mL)	0	0	0	0	0	0	1	3	5	0	0	0
Parijat (0.01% methanolic solution) (mL)	0	0	0	0	0	0	0	0	0	1	3	5

Table 2. Angle of Repose and flow properties

Angle of Repose (°)	**Type of Flow**
< 20	Excellent
20 – 30	Good
30 – 34	Passable
> 34	Very Poor

Table 3. Hausner's ratio

Flow properties	**Hausner's ratio**
Excellent/ Very Free Flow	1-1.11
Good/ Free Flow	1.12-1.18
Fair	1.19-1.25
Passable	1.26-1.34
Poor Flow/ Cohesive	1.35-1.45
Very Poor Flow/ Very Cohesive	1.46-.159
Approximate no Flow	>1.6

Table 4. Carr's Compressibility index

Flow properties	**Carr's index**
Excellent/ Very Free Flow	<10
Good/ Free Flow	1 - 15.0
Fair	16-20
Passable	24-25
Poor Flow/ Cohesive	26-31
Very Poor Flow/ Very Cohesive	32-37
Approximate no Flow	>38

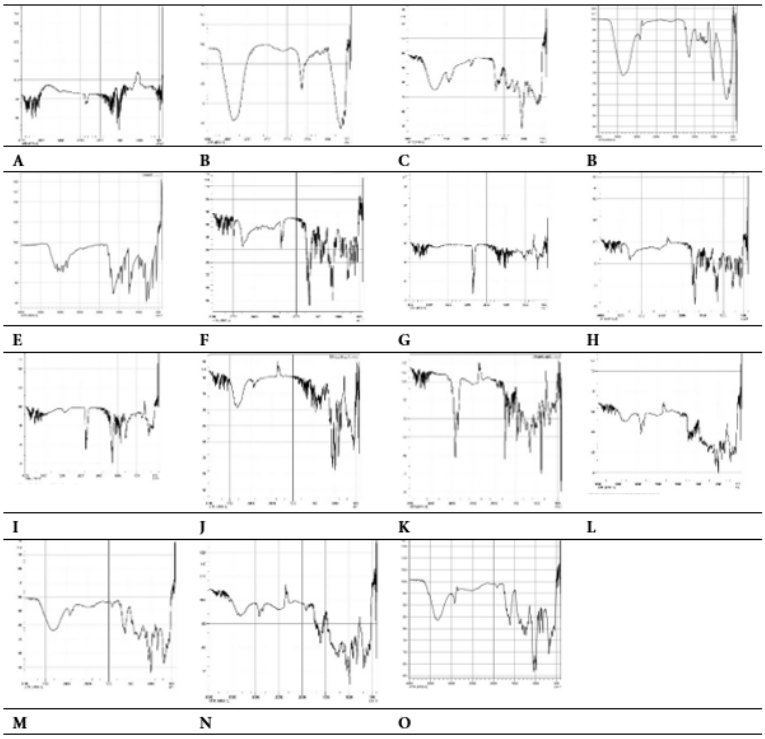

Figure 1. FTIR of (A) Curcumin, (B) Amaranth, (C) Pigment obtained from *Opuntia ficus-indica* fruits, (D) Pigment obtained from *Nyctanthes arbor-tristis* flowers, (E) 5FU, (F) Citric acid**, (G)** Sodium bicarbonate, (H) Sodium stearate, (I) Polyvinylpyrrolidone, (J) Sucrose, (K) Lemon oil, (L) FDT using curcumin, (M) FDT using amaranth, (N) FDT using opuntia, (O) FDT using Parijat

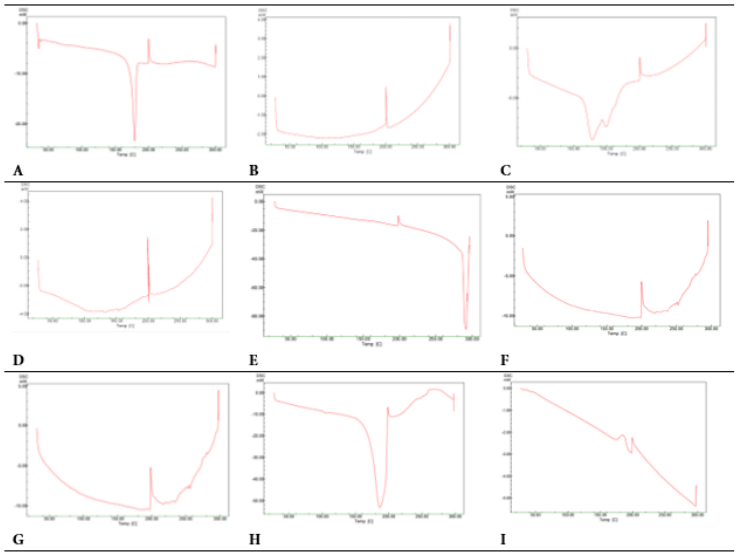

Figure 2. DSC of (A) Curcumin, (B) Amaranth, (C) *Opuntia ficus-indica* fruits pigment, (D) *Nyctanthes arbor-tristis* flowers pigment, (E) 5FU, (F) FDT using curcumin, (G) FDT using amaranth, (H) FDT using opuntia, (I) FDT using Parijat

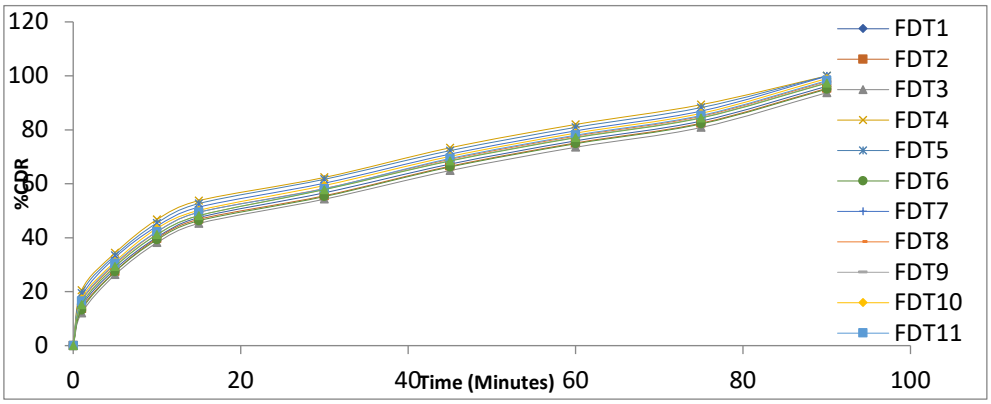

Figure 3. Graph of *in-vitro* drug release from FDTs

Table 5. Bulk characterization of powder to prepare FDT

Formulation	FDT1	FDT2	FDT3	FDT4	FDT5	FDT6	FDT7	FDT8	FDT9	FDT10	FDT11	FDT12
Bulk density	0.65±0.24	0.64±0.23	0.63±0.22	0.62±0.23	0.64±0.23	0.63±0.24	0.61±0.22	0.63±0.23	0.64±0.23	0.62±0.43	0.62±0.22	0.63±0.24
Tapped density	0.79±0.46	0.77±0.42	0.76±0.36	0.82±0.15	0.78±0.73	0.78±0.43	0.80±0.35	0.78±0.64	0.79±0.41	0.78±0.52	0.78±0.36	0.78±0.43
Void volume	1.10±0.25	1.20±0.25	1.20±0.46	0.90±0.25	1.10±0.34	1.10±0.33	1.00±0.26	1.10±0.24	1.10±0.22	1.10±0.63	1.10±0.16	1.10±0.46
Porosity	0.26±0.63	0.29±0.35	0.30±0.36	0.21±0.34	0.26±0.56	0.26±0.65	0.25±0.52	0.26±0.56	0.26±0.42	0.27±0.25	0.27±0.46	0.26±0.26
Angle of repose (θ)	27.24±0.26	27.62±0.63	26.34±0.26	24.77±0.53	27.62±0.38	28.07±0.36	26.34±0.38	27.84±0.53	22.54±0.34	24.36±0.45	24.56±0.36	29.05±0.21
Carr's index	17.63±0.63	16.65±0.24	16.95±0.34	24.57±0.73	18.82±0.23	18.89±0.22	22.93±0.32	18.97±0.14	18.93±0.12	20.21±0.72	20.99±0.26	19.96±0.16
Hausner's index	1.21±0.47	1.20±0.58	1.20±0.44	1.32±0.25	1.23±0.14	1.23±0.17	1.29±0.24	1.23±0.43	1.23±0.45	1.25±0.36	1.26±0.53	1.24±0.46

Table 6. Evaluation parameter of FDT

Formulation	FDT1	FDT2	FDT3	FDT4	FDT5	FDT6	FDT7	FDT8	FDT9	FDT10	FDT11	FDT12
Thickness	4.41±0.24	4.41±0.53	4.41±0.76	4.41±0.23	4.40±0.45	4.41±0.26	4.41±0.42	4.41±0.52	4.41±0.16	4.41±0.25	4.41±0.21	4.41±0.36
Hardness	3.43±0.56	3.48±0.23	3.43±0.34	3.42±0.53	3.44±0.25	3.42±0.43	3.41±0.63	3.42±0.26	3.52±0.22	3.94±0.15	3.44±0.42	3.73±0.31
Friability (%)	0.39±0.25	0.39±0.32	0.39±0.46	0.39±0.64	0.39±0.62	0.38±0.35	0.39±0.35	0.39±0.24	0.39±0.24	0.39±0.23	0.39±0.27	0.38±0.35
Weight variation	301.14±0.22	301.17±0.56	301.25±0.25	300.23±0.23	301.45±0.11	302.11±0.22	300.82±0.43	299.98±0.35	301.12±0.53	301.24±0.43	301.27±0.34	300.24±0.53
Water absorption ratio	77±0.35	74±0.22	69±0.34	89±0.46	85±0.54	82±0.16	84±0.22	78±0.45	73±0.12	79±0.34	75±0.63	68±0.23
Wetting time (Seconds)	41±0.74	53±0.42	59±0.43	11±0.22	18±0.15	22±0.32	14±0.15	21±0.14	28±0.23	31±0.12	32±0.22	49±0.42
Drug content	99.97±0.25	99.98±0.14	98.91±0.33	99.94±0.15	99.96±0.35	99.92±0.41	98.93±0.25	98.91±0.22	99.94±0.53	98.96±0.16	98.98±0.34	98.92±0.53
In-vitro disintegration time (Seconds)	11±0.15	15±0.21	9±0.34	11±0.45	11±0.23	14±0.64	23±*0.35	17±0.43	13±0.14	27±0.35	11±0.33	10±0.45

Table 7. Stability study of optimized FDT batch

Days	Drug content	Wetting time (sec)	Disintegration time (Sec)
7	99.99±1.23	11±2.23	11.43±1.53
14	99.52±1.34	13±4.64	13.74±1.84
21	98.97±0.45	16±3.15	14.33±1.26
28	98.67±1.54	18±5.63	15.56±1.32

Table 8. *In-vitro* drug release study

Time (Minutes)	FDT1	FDT2	FDT3	FDT4	FDT5	FDT6	FDT7	FDT8	FDT9	FDT10	FDT11	FDT12
1	14.47±0.12	13.69±0.39	12.08±0.53	20.51±0.25	19.46±0.20	13.14±0.12	18.13±0.21	16.21±0.44	15.29±0.30	17.32±0.24	16.51±0.14	15.21±0.23
5	26.37±0.39	24.54±0.50	23.28±0.26	34.34±0.27	33.46±0.42	28.40±0.48	32.63±0.31	30.05±0.18	29.27±0.17	31.13±0.13	30.52±0.13	29.32±0.37
10	40.13±0.32	39.73±0.41	38.13±0.46	46.72±0.31	45.46±0.19	39.23±0.33	44.25±0.32	42.15±0.49	41.17±0.23	43.43±0.45	42.21±0.25	41.15±0.26
15	47.47±0.15	46.82±0.19	45.28±0.27	53.74±0.18	52.66±0.34	46.30±0.14	51.33±0.21	49.42±0.31	48.16±0.36	50.13±0.14	49.42±0.18	48.18±0.13
30	56.65±0.47	55.56±0.52	54.28±0.36	62.35±0.54	61.66±0.21	55.25±0.20	60.22±0.28	58.24±0.19	57.93±0.51	59.35±0.12	58.16±0.28	57.81±0.24
45	67.28±0.38	66.5±0.33	64.89±0.49	73.33±0.34	72.27±0.55	66.21±0.56	70.99±0.22	69.05±0.58	68.6±0.44	70.14±0.29	69.37±0.16	68.42±0.45
60	75.91±0.38	75.13±0.29	73.52±0.15	81.98±0.23	80.9±0.43	74.84±0.35	79.62±0.12	77.68±0.25	77.23±0.59	78.77±0.41	78.03±0.29	77.05±0.31
75	83.25±0.16	82.47±0.37	80.86±0.11	89.32±0.35	88.24±0.48	82.18±0.22	86.96±0.57	85.02±0.17	84.57±0.46	86.11±0.26	85.34±0.15	84.39±0.42
90	96.14±0.51	95.36±0.17	93.75±0.28	99.98±0.24	99.96±0.43	95.07±0.34	99.85±0.47	97.91±0.22	97.46±0.17	99.01±0.16	98.23±0.13	97.28±0.27

Table 9. Drug release kinetics of FDT

	1		2		3		4		5		6		7		8		9		10		11		12	
Model Fitting	R^2	K	R^2	k	R^2	k	R^2	k	R^2	k	R^2	k	R^2	k	R^2	k	R^2	k	R^2	k	R^2	k	R^2	k
Zero order	0.8917	0.8952	0.8944	0.8945	0.8989	0.8877	0.8586	0.8959	0.8656	0.8981	0.8926	0.8832	0.8735	0.8994	0.8823	0.8949	0.8876	0.8986	0.8788	0.8989	0.8833	0.8971	0.8870	0.8962
1st order	0.9041	-0.0282	0.9155	-0.0269	0.9322	-0.0248	0.6419	-0.0611	0.6549	-0.0566	0.9173	-0.0264	0.6977	-0.0483	0.8612	-0.0322	0.8762	-0.0310	0.8088	-0.0369	0.8497	-0.0333	0.8805	-0.0305
Higuchi Matrix	0.9130	10.0601	0.9142	10.0369	0.9159	9.9612	0.9100	10.1914	0.9099	10.1821	0.9130	9.9743	0.9098	10.1633	0.9110	10.1013	0.9117	10.0998	0.9102	10.1424	0.9105	10.1155	0.9118	10.0868
Peppas	0.9933	3.1986	0.9904	3.1158	0.9906	2.9794	0.9954	3.7067	0.9956	3.6302	0.9931	3.1448	0.9951	3.5377	0.9949	3.3773	0.9956	3.3012	0.9951	3.4632	0.9952	3.4001	0.9954	3.2983
Hix.Crow.	0.9545	0.0060	0.9571	0.0059	0.9609	0.0056	0.8985	0.0079	0.8954	0.0078	0.9565	0.0058	0.8998	0.0074	0.9428	0.0064	0.9481	0.0063	0.9297	0.0068	0.9406	0.0065	0.9486	0.0063
Parameters for Korsmeyer-Peppas Equation **n**	0.4100		0.4225		0.4438		0.3428		0.3523		0.4176		0.3640		0.3847		0.3963		0.3734		0.3814		0.3965	
k	3.1986		3.1158		2.9794		3.7067		3.6302		3.1448		3.5377		3.3773		3.3012		3.4632		3.4001		3.2983	
Best fit model	Peppas Korsmeyer		Peppas Korsmeyer		Peppas Korsmeyer		Peppas Korsmeyer		Peppas Korsmeyer		Peppas Korsmeyer		Peppas Korsmeyer		Peppas Korsmeyer		Peppas Korsmeyer		Peppas Korsmeyer		Peppas Korsmeyer		Peppas Korsmeyer	
Mechanism of release	Fickian Diffusion (Higuchi Matrix)		Fickian Diffusion (Higuchi Matrix)		Fickian Diffusion (Higuchi Matrix)		Fickian Diffusion (Higuchi Matrix)		Fickian Diffusion (Higuchi Matrix)		Fickian Diffusion (Higuchi Matrix)		Fickian Diffusion (Higuchi Matrix)		Fickian Diffusion (Higuchi Matrix)		Fickian Diffusion (Higuchi Matrix)		Fickian Diffusion (Higuchi Matrix)		Fickian Diffusion (Higuchi Matrix)		Fickian Diffusion (Higuchi Matrix)	

The FTIR of lemon oil showed the presence of alkyne C-H bend at 614 cm^{-1}, 639 cm^{-1}, cis C-H out of plan bend at 759 cm^{-1}, C-H out of plan at 797 cm^{-1}, C-H out of plan bending 914 cm^{-1}, trans C-H out of plan at 956 cm^{-1}, C-O stretch 1115 cm^{-1}, 1155 cm^{-1}, 1147 cm^{-1}, 1198, aromatic C-H in plan bend at 1230 cm^{-1}, O-H in-plan bend at 1278 cm^{-1}, C-H Bend at 1310 cm^{-1}, 1331 cm^{-1}, C-H *sym/asym* bend at 1376 cm^{-1}, 1436 cm^{-1}, C=C stretch at 1644 cm^{-1}, C=C stretch at 1681 cm^{-1}, alkyl carbonate at 1746 cm^{-1}, aldehyde CHO- at 2726 cm^{-1}, C-H *sym/asym str* at 2856 cm^{-1}, 2835 cm^{-1}, 2918 cm^{-1}, 2964 cm^{-1}, C=C-C aromatic ring stretch at 3008 cm^{-1}, 3072 cm^{-1}.

The DSC of 5-FU, citric acid, sodium bicarbonate, sodium stearate, polyvinylpyrrolidone, sucrose, lemon oil, curcumin, amaranth, pigment from *Opuntia ficus-indica* fruits and pigment from *Nyctanthes arbor-tristis* flowers showed no drug excipient interaction as shown in is shown in Figure-3. The DSC of curcumin showed endothermic peak at 180^{0}C and exothermic peak 200^{0}C, amaranth, showed exothermic peak at 200^{0}C, *Opuntia ficus-indica* fruits pigment showed endothermic peak at 130^{0}C and 160^{0}C while exothermic at 200^{0}C, *Nyctanthes arbor-tristis* flowers pigment showed exothermic at 200^{0}C, 5FU showed exothermic peak at 200^{0}C and endothermic peak at 290^{0}C, FDT using curcumin showed exothermic peak at 200^{0}C, FDT using amaranth showed exothermic peak at 200^{0}C, FDT using opuntia showed endothermic peak at 190^{0}C and exothermic peak at 200^{0}C, FDT using Parijat showed exothermic peak at 180^{0}C, 200^{0}C and endothermic peak at 199^{0}C.

The drug *5-FU* was free flowing white crystalline powder with irritating taste and unpleasant odor. The melting point of 5-Fluorouracil was found to be 282 ± 0.51˚C and reported value was 282-283˚C, loss on drying was found to be 0.0014%. The UV Spectrophotometric study showed the maximum absorbance (λ_{max}) of 5-FU was 266 nm in phosphate buffer (pH 7.4). The calibration data showed in Table-5 and calibration curve plotted against absorbance and concentration in Figure-4.

The excipients found to be compatible with the drug 5FU by FTIR and DSC studies as shown in Figure-2 and Figure-4, respectively. The FTIR of FDT contain curcumin as coloring agent showed the presence of OH, CH, Ar C=C, C-F, C=O, C-N, N-H, phenolic C-O, O-H (COOH), C=O (COOH), C-C, N-C=O, CH_2, C-F, C-OH stretching and C-OH bending, metal-carboxylate and carboxylic acid, COO^- stretching, methyl, esters group.

The FTIR of FDT contain amaranth as coloring agent showed the presence of aromatic C=C, C-O, C=O, OH, C-H, C–OH, C-S, -N=N-, C=C-C Aromatic ring stretch, C–C, C-F, C-N, N-H, O-H (COOH), C=O (COOH), C-OH, metal-carboxylate and carboxylic acid, COO^- stretching, methyl, esters.

The FTIR of FDT contain opuntia as coloring agent showed the presence of C-H, C=C, C=C-C Aromatic ring stretch, OH stretch, C–O stretch, C-S stretch, C-OH stretching, C=O, aromatic C=C, C-F, C=O, C-N, N-H, O-H (COOH), C=O (COOH), C-OH stretching, C-OH bending, metal-carboxylate and carboxylic acid (1698-1710 cm^{-1}, COO^- stretching, C-C, N-C=O, methyl, esters.

The FTIR of FDT contain Parijat as coloring agent showed the presence of C-H stretch, aromatic C=C, C=C-C Aromatic ring stretch, OH stretch, C-C, C-O stretch, Aromatic C-H in-plane bend, aromatic C-H out-of-plane bend, C-S stretch, C-OH stretching, C-O stretch, C=O, C-F, C-N, N-H, O-H (COOH), C=O (COOH), metal-carboxylate and carboxylic acid, C-H stretching, COO^- stretching, methyl, esters.

The different powder blends to prepare various batches of FDT showed and derived properties of bulk powder blends showed in Table 6. The evaluation parameters of FDT showed in Table 7. The wetting time of FDT was shorter at low pigment concentration and longer at high pigment concentration in both cases whether pigment is hydrophilic or hydrophobic in nature. The wetting time of FDT3 and FDT2 showed the longest wetting time among all FDT batches due to the use of higher concentration of hydrophobic colorant curcumin as the hydrophobic colorant adsorb on surface of crystal lattice of 5-FU and sucrose that inhibit wetting of crystal. The use of hydrophilic colorant at high concentration also showed an increase in wetting time due to inhibit wetting and dissolution of crystal faces. The order of wetting time was FDT4 < FDT7 < FDT5 < FDT8 < FDT6 < FDT9 < FDT10 < FDT11 < FDT1 < FDT12 < FDT2 < FDT3. Water absorption ratio was more with hydrophilic colorant than hydrophobic colorant. The order of water absorption ratio was FDT12 < FDT3 < FDT9 < FDT2 < FDT11 < FDT1 < FDT8 < FDT10 < FDT6 < FDT7 < FDT5 < FDT4. The order of *in-vitro* disintegration time was maximum for FDT batch FDT3 as high concentration of hydrophobic pigment curcumin used, and maximum drug release was found with FDT12 as hydrophilic pigment used. The *in-vitro* drug release studies conducted up to 90 minutes showed the variation in drug release form 93.75±0.28-99.98±0.24 % as shown in Table 8, Figure 5. The use of hydrophilic pigment at low concertation showed maximum drug release within 90 minutes showed by batch FDT4. The order of drug release was FDT3 < FDT6 < FDT2 < FDT1 < FDT12 < FDT9 < FDT8 < FDT11 < FDT10 < FDT7 < FDT5 < FDT4. The results of ANOVA test showed in Table 9 suggest the difference between the sample averages of all groups is not big enough to be statistically significant. All FDT showed the Peppas Korsmeyer model as the best fit model. A study by Mushtaq et al, 2021, Rozhan et. al., 2023 also found the best fit model for drug release from FDT was Korsmeyer-Peppas model. The result of drug release kinetics was similar. The mechanism of drug release was Fickian diffusion (Higuchi Matrix) as showed in Table 10. The best selected batch FDT4 selected to conduct stability study and drug content, wetting time, disintegration time evaluated at 25±2^{0}C, 60±5%RH (ICH zone-II,

mediterranean/subtropical zone) and result was tabulated in Table-11.

4. Conclusion

The FDT batches prepared successfully by direct compression method. All batches showed Peppas Korsmeyer model as the best fit model and the mechanism of drug release was Fickian Diffusion (Higuchi Matrix). The drug release kinetics resembles with study by Mushtaq et al, 2021, Rozhan et. Al., 2023 where Korsmeyer-Peppas model was the best fit model and Fickian Diffusion (Higuchi Matrix) was the mechanism of drug release. As different pigments used to determine the effect of different colorants on drug release, it was found that among hydrophilic colorants, the most aqueous soluble color showed the faster drug release and the order of aqueous solubility of hydrophilic colorant was found in following order: Amaranth > Pigment form Opuntia > Pigment form Parijat > Curcumin. The use of hydrophilic or hydrophilic pigment at low concertation showed maximum drug release within 90 minutes and batch FDT4 showed maximum drug release. Least drug release showed by FDT3 that utilized highest concentration of hydrophobic pigment that hampers dissolution by adsorption of pigment of solid surfaces. The high concentrations of aqueous soluble pigments also retard the drug dissolution and drug release due to their adsorption on crystal faces. The hydrophobic colorant retards the dissolution of drug as compared to hydrophilic colorants. The ANOVA test results suggest the difference between the sample averages of all groups is not big enough to be statistically significant. All FDT showed the Peppas Korsmeyer model as the best fit model and the mechanism of drug release was Fickian diffusion. The best selected batch FDT4 showed drug content 98.67±1.54, Wetting time 18±5.63 seconds and Disintegration time 15.56±1.32 Seconds at after 28 days at 25±2^{o}C, 60±5%RH (ICH zone-II, mediterranean/subtropical zone).

Symbols and Abbreviations

PVP. polyvinyl pyrrolidone; **FDT.** Fast-dissolving tablets; **sec.** Second; **L.** Litre; **mL.** Milliliter; **Min.** Minutes; **AR.** Analytical Reagent; **U.V.**. Ultraviolet; **µ.** Micro; **g.** Gram; **FTIR.** Fourier transform infrared; **ρ.** Density; **θ.** Theta; **I.P.** Indian Pharmacopoeia; **%.** Percentage; **N.** Normal; **°.** Degree; **C.** Centigrade; **RH.** Relative humidity; **CI.** Carr's index or compressibility index; **ANOVA.** Analysis of variance.

Author contributions

E.T.B., S.V., D.K., S.A., A.H., S.A.R., S.B., A.O. conceptualized, performed fieldwork, analyzed data, drafted the original manuscript, reviewed and edited it.

Acknowledgment

The authors were grateful to the management of TIU to provide every facility for the conduct of this research.

Competing financial interests

The authors have no conflict of interest.

References

Arif, R., Visht, S., Yassen, A.O., Salih, S.S., 2024. Optimizing Fast-Dissolving Tablets of Ketotifen. Impact of Sodium Bicarbonate and Citric Acid in Formulation and Evaluation, Journal of Angiotherapy, 8(1), 1-11, 9379.

Aulton, M. and Taylor, K., 2013. Aulton's pharmaceutics. Edinburgh: Churchill Livingstone.

Ayenew, Z., Puri, V., Kumar, L. and Bansal, A., 2009. Trends in Pharmaceutical Taste Masking Technologies: A Patent Review. Recent Patents on Drug Delivery & Formulation, 3(1), pp.26-39.

Balata, G., Zidan, A., Abourehab, M. and Essa, E., 2016. Rapid disintegrating tablets of simvastatin dispersions in polyoxyethylene–polypropylene block copolymer for maximized disintegration and dissolution. Drug Design, Development and Therapy, Volume 10, pp.3211-3223.

Bharkatiya, M., Kitawat, S. and Gaur, K., 2018. Formulation and Characterization of Fast Dissolving Tablet of Salbutamol Sulphate. American Journal of Pharmacological Sciences, 6(1), pp.1-6.

Bhimte, N. and Tayade, P., 2007. Evaluation of microcrystalline cellulose prepared from sisal fibers as a tablet excipient: A technical note. AAPS PharmSciTech, 8(1), pp.E56-E62.

BI, Y., Sunada, H., Yonezawa, Y., Danjo, K., Otsuka, A. and Iida, K., 1996. Preparation and Evaluation of a Compressed Tablet Rapidly Disintegrating in the Oral Cavity. Chemical and Pharmaceutical Bulletin, 44(11), pp.2121-2127.

Bijauliya, R., Kannojia, P., Mishra, P., Singh, P. and Kannaujia, R., 2021. Pharmacognostical and Physiochemical Study on the Leaves of Nyctanthes arbor-tristis Linn. Journal of Drug Delivery and Therapeutics, 11(4), pp.30-34.

Bond, C., 1998. Comparison of Buccal and Oral Prochlorperazine in the Treatment of Dizziness Associated with Nausea and/or Vomiting. Current Medical Research and Opinion, 14(4), pp.203-212.

Corveleyn, S. and Remon, J., 1997. Formulation and production of rapidly disintegrating tablets by lyophilisation using hydrochlorothiazide as a model drug. International Journal of Pharmaceutics, 152(2), pp.215-225.

Fernández-López, J., Giménez, P., Angosto, J. and Moreno, J., 2022. A Process of Recovery of a Natural Yellow Colourant from Opuntia Fruits.

Hajjar, E., Cafiero, A. and Hanlon, J., 2007. Polypharmacy in elderly patients. The American Journal of Geriatric Pharmacotherapy, 5(4), pp.345-351.

Heer, S., Jindal, S., Mishra, G., Madan, J., Gupta, G., AWASTHI, D., Pinto, T., Dua, K. and Kulkarni, G., 2019. Formulation and characterization of oral rapid disintegrating tabletsof levocetirizine. Polymers in Medicine, 48(1), pp.31-40.

Hirlekar, R. and Kadam, V., 2009. Preformulation Study of the Inclusion Complex Irbesartan-β-Cyclodextrin. AAPS PharmSciTech, 10(1), pp.276-281.

Kozarewicz, P., 2014. Regulatory perspectives on acceptability testing of dosage forms in children. International Journal of Pharmaceutics, 469(2), pp.245-248.

Kulkarni, G.T. and Visht S., 2015:. Effect of some cations as counter ions on ulcer healing activity of glycyrrhetinic acid on male albino rats.. Int. J. Chem. Sci. , 13((3);), pp. 1511-1521..

Kumar, M. Visht, S. Ali, S. Agarwal, S. Bhola, A. Preparation and evaluation of fast dissolving drug delivery system containing levocetrizine HCl.. Int. J. Pharm. Sci. , 2((3);), pp. 109-111..

Mahant, S.A. Gaidhane, A.K. Dokrimare, N.A. Wadher, K.J. Lohiya, R.T. Umekar, M.J., 2020. Formulation and Evaluation of Fast Dissolving Tablet of Montelukast Sodium: Effect of Superdisintegrants. Scholars Academic Journal of Pharmacy, 09(02), pp.86-89.

Mehra, P., Kapoor, V., Gupta, N., Singh Rajpoot, D. and Sharma, N., 2021. Formulation Evaluation and Characterization of Fast Dissolving Tablets of Rofecoxib. Research Journal of Topical and Cosmetic Sciences, pp.60-64.

Mohan, A. and Gundamaraju, R., 2015. In vitro and in vivo evaluation of fast-dissolving tablets containing solid dispersion of lamotrigine. International Journal of Pharmaceutical Investigation, 5(1), p.57.

Nagar, P. Chauhan, K.S., I. Verma, M. Yasir, M. Khan, A. Sharma, R. Gupta, N. 2011. Orally disintegrating tablets : Formulation, preparation techniques and evaluation.. J. App Pharm Sci. , 01((04);), pp. 35-45..

Ngamwonglumlert, L., Devahastin, S. and Chiewchan, N., 2017. Natural colorants: Pigment stability and extraction yield enhancement via utilization of appropriate pretreatment and extraction methods. Critical Reviews in Food Science and Nutrition, 57(15), pp.3243-3259.

Open Library. 2022. European Pharmacopoeia 5th Ed. Main Volume 5.0, 2005 with Supplements 5.1 and 5.2 (European Pharmacopoeia) (July 2004 edition)

Panigrahi, R. and Behera, S., 2022. A Review On Fast Dissolving Tablets.Webmedcentral.com.

Parkash, V., Maan, S., Deepika, Yadav, S., Hemlata and Jogpal, V., 2011. Fast disintegrating tablets: Opportunity in drug delivery system. Journal of Advanced Pharmaceutical Technology & Research, 2(4), p.223.

Patel, Z., bhura, R. and Shah, S., 2020. Formulation optimization and evaluation of mouth dissolving film of ramosetron hydrochloride. International Journal of Current Pharmaceutical Research, pp.99-106.

Rai, R. Visht, S. Khan, A. Saini, P., 2012: . Formulation and Evaluation of 5-Fluorouracil Loaded Liposomes.. Int.J.Pharm.Phytopharmacol.Res. , 2((3);), pp. 222-228..

Ratner, P., Lim, J. and Georges, G., 2000. Comparison of once-daily ebastine 20 mg, ebastine 10 mg, loratadine 10 mg, and placebo in the treatment of seasonal allergic rhinitis. Journal of Allergy and Clinical Immunology, 105(6), pp.1101-1107.

Sandhyarani, G., Srivastava,, P., Malviya,, R. and Visht, S., 2010. Formulation and evaluation of atenolol oral disintegrating tablets. World Journal of Pharmaceutical Research, pp.1073-1079.

Santos López, E., 2022. Colorant extraction from red prickly pear (Opuntia lasiacantha) for food application.

Scarano, P., Naviglio, D., Prigioniero, A., Tartaglia, M., Postiglione, A., Sciarrillo, R. and Guarino, C., 2020. Sustainability: Obtaining Natural Dyes from Waste Matrices Using the Prickly Pear Peels of Opuntia ficus-indica (L.) Miller. Agronomy, 10(4), p.528.

Sepúlveda, E., Sáenz, C., Aliaga, E. and Aceituno, C., 2007. Extraction and characterization of mucilage in Opuntia spp. Journal of Arid Environments, 68(4), pp.534-545.

Sharma, D., 2012. Fast disintegrating tablets: a review on an emerging trend in novel oral drug delivery technology and new market opportunities. Journal of Drug Delivery and Therapeutics, 2(3).

Sharma, D., 2013. Formulation Development and Evaluation of Fast Disintegrating Tablets of Salbutamol Sulphate for Respiratory Disorders. ISRN Pharmaceutics, 2013, pp.1-8.

Sharma, S., Sharma, N. and Gupta, G., 2010. Formulation of Fast-Dissolving Tablets of Promethazine Theoclate. Tropical Journal of Pharmaceutical Research, 9(5).

Shirsand, S., Suresh, S., Swamy, P., Para, M. and Nagendra Kumar, D., 2010. Formulation design of fast disintegrating tablets using disintegrant blends. Indian Journal of Pharmaceutical Sciences, 72(1), p.130.

Shrivastava, R. and Bharadwaj, A., 2018. Nyctanthes arbortristis an Important Medicinal Plant of Madhya Pradesh State - A Review. Pharmaceutical and Biosciences Journal, pp.10-15

Singh, J., Singh, A. and Singh, A., 2021. Nyctanthes arbor-tristis: a comprehensive review. World Journal of Current Medical and Pharmaceutical Research, pp.74-78.

Soni, T., Nagda, C., Gandhi, T. and Chotai, N., 2008. Development of Discriminating Method for Dissolution of Aceclofenac Marketed Formulations. Dissolution Technologies, 15(2), pp.31-35.

Tawashi, R. and Piccolo, J., 1972. Inhibited dissolution of drug crystals by certified water-soluble dyes: in vivo effect. Journal of Pharmaceutical Sciences, 61(11), pp.1857-1858.

Tripathi, S. and K. Tripathi, P., 2012. Evaluation of Anxiolytic Effect in Flowers of Nyctanthes arbor-tristis. Journal of Current Pharma Research, 3(1), pp.709-717.

Tumuluri, V., 2022. Pharmaceutical mini-tablets.

Überall, M. and Müller-Schwefe, G., 2011. S615 Sublingual fentanyl tablet for breakthrough cancer pain: dose titration in daily practice. European Journal of Pain Supplements, 5(1), pp.273-274.

Visht, S. and Kulkarni, G., 2015. Studies on the preparation and in vitro - in vivo evaluation of mucoadhesive microspheres of glycyrrhetinic acid isolated from liquorice. Bangladesh Pharmaceutical Journal, 18(1), pp.30-37.

Visht, S. and T. Kulkarni, G., 2016. Glycyrrhetinic Acid Ammonium Loaded Microspheres Using Colocasia esculenta and Bombax ceiba mucilages: In Vitro and In Vivo Characterization. Current Drug Therapy, 11(2), pp.101-114.

Visht, S., Anjum, N. and Saini, A., 2018. Comparison of drug release: microparticles vs nanoparticles. International Research Journal of Pharmacy, 9(4), pp.52-58.

Wolska, E., Sznitowska, M., Krzemińska, K. and Ferreira Monteiro, M., 2020. Analytical Techniques for the Assessment of Drug-Lipid Interactions and the Active Substance Distribution in Liquid Dispersions of Solid Lipid Microparticles (SLM) Produced de novo and Reconstituted from Spray-Dried Powders. Pharmaceutics, 12(7), p.664.

Zade, P.S., Kawtikwar, PS. Sakarkar, DM., 2022. Formulation, Evaluation and Optimization of Fast Dissolving Tablet Containing Tizanidine Hydrochloride. International Journal of Pharm Tech Research, 1, 34-42. - References - Scientific Research Publishing.

Zhang, H., Zhang, J. and Streisand, J., 2002. Oral Mucosal Drug Delivery. Clinical Pharmacokinetics, 41(9), pp.661-680.